Published in final edited form as:
Glia. 2003 December ; 44(3): 205–218.

Coupling of Astrocyte Connexins Cx26, Cx30, Cx43 to Oligodendrocyte Cx29, Cx32, Cx47: Implications From Normal and Connexin32 Knockout Mice

J.I. NAGY[1,*], **A.-V. IONESCU**[1], **B.D. LYNN**[1], and **J.E. RASH**[2]

1 *Department of Physiology, Faculty of Medicine, University of Manitoba, Winnipeg, Manitoba, Canada*

2 *Department of Anatomy and Neurobiology and Program in Molecular, Cellular and Integrative Neurosciences, Colorado State University, Fort Collins, Colorado*

Abstract

Oligodendrocytes in vivo form heterologous gap junctions with astrocytes. These oligodendrocyte/astrocyte (A/O) gap junctions contain multiple connexins (Cx), including Cx26, Cx30, and Cx43 on the astrocyte side, and Cx32, Cx29, and Cx47 on the oligodendrocyte side. We investigated connexin associations at A/O gap junctions on oligodendrocytes in normal and Cx32 knockout (KO) mice. Immunoblotting and immunolabeling by several different antibodies indicated the presence of Cx32 in liver and brain of normal mice, but the absence of Cx32 in liver and brain of Cx32 KO mice, confirming the specificity and efficacy of the antibodies, as well as allowing the demonstration of Cx32 expression by oligodendrocytes. Oligodendrocytes throughout brain were decorated with numerous Cx30-positive puncta, which also were immunolabeled for both Cx32 and Cx43. In Cx32 KO mice, astrocytic Cx30 association with oligodendrocyte somata was nearly absent, Cx26 was partially reduced, and Cx43 was present in abundance. In normal and Cx32 KO mice, oligodendrocyte Cx29 was sparsely distributed, whereas Cx47-positive puncta were densely localized on oligodendrocyte somata. These results demonstrate that astrocyte Cx30 and oligodendrocyte Cx47 are widely present at A/O gap junctions. Immunolabeling patterns for these six connexins in Cx32 KO brain have implications for deciphering the organization of heterotypic connexin coupling partners at A/O junctions. The persistence and abundance of Cx43 and Cx47 at these junctions after Cx32 deletion, together with the paucity of Cx29 normally present at these junctions, suggests Cx43/Cx47 coupling at A/O junctions. Reductions in Cx30 and Cx26 after Cx32 deletion suggest that these astrocytic connexins likely form junctions with Cx32 and that their incorporation into A/O gap junctions is dependent on the presence of oligodendrocytic Cx32.

Keywords

connexin30; connexin29; connexin32; connexin47; immunohistochemistry

INTRODUCTION

Neurons, astrocytes, and ependymocytes in the CNS form extensive homologous gap junctions (e.g., astrocyte-to-astrocyte [A/A] junctions), whereas oligodendrocytes form only heterologous gap junctions with astrocytes (A/O junctions), but also form autologous junctions

*Correspondence to: J.I. Nagy, Department of Physiology, Faculty of Medicine, University of Manitoba, 730 William Avenue, Winnipeg, Manitoba, Canada R3E 3J7. E-mail: nagyji@ms.umanitoba.ca.

Grant sponsor: Canadian Institutes of Health Research; Grant sponsor: National Institutes of Health; Grant number: NS-31027; Grant number: NS-44010; Grant number: NS-44395.

between myelin layers. Few if any gap junctions occur between two oligodendrocytes; however, oligodendrocytes indirectly communicate with each other through gap junctions with astrocyte "intermediaries" (Mugnaini, 1986; Wolburg and Rohlmann, 1995; Rash et al., 1997, 2001). Several different members of the connexin (Cx) family of proteins (Willecke et al., 2002) contribute to gap junctional intercellular communication (GJIC) at the gap junctions linking each macroglial cell type. These include Cx26, Cx30, and Cx43 in astrocytes (Yamamoto et al., 1990a,b; Nagy et al., 1997, 1999, 2001) and Cx29, Cx32, and Cx47 in oligodendrocytes (Dermietzel et al., 1997; Kunzelmann et al., 1997; Altevogt et al., 2002; Nagy et al., 2003a,b). A related but controversial issue is whether Cx32 is expressed exclusively by oligodendrocytes as reported by us (Li et al., 1997; Rash et al., 2001), or whether Cx32 is additionally expressed by neurons as reported by others (reviewed in Nagy et al., 2003a). Thin-section electron microscopy (EM) and freeze-fracture replica immunogold labeling (FRIL) studies have indicated that the three astrocytic connexins Cx26, Cx30, and Cx43 are each incorporated not only into individual A/A junctions, but also into the astrocyte side of A/O junctions (Nagy et al., 1999; Rash et al., 2001). Although relationships between Cx30 and oligodendrocytes have yet to be examined by light microscopy (LM), punctate labeling for astrocytic Cx26 and Cx43 was demonstrated around oligodendrocyte somata, and this labeling was co-associated with oligodendrocytic Cx32 (Rash et al., 2001; Nagy et al., 2001). Because the set of connexins in astrocytes is completely different from the set of connexins in oligodendrocytes, A/O gap junctions are necessarily heterotypic, meaning that connexins forming connexons in astrocytes couple with entirely different connexin constituents in oligodendrocytes. Some connexin coupling pairs are permissive for the formation of functional GJIC channels (e.g., Cx30/Cx32), while others are not (Cx43/Cx32) (White and Bruzzone, 1996). Nevertheless, the specific connexin pairing combinations that occur at A/O junctions are completely unknown.

The aims of this study were threefold. First, immunolabeling patterns of Cx32 in wild-type (WT) and Cx32 knockout (KO) mice were investigated to confirm specificities of anti-Cx32 antibodies, as well as to confirm positive Cx32 localization in CNS of WT animals. Second, the relative association of astrocyte Cx30 with oligodendrocyte Cx32 was investigated by LM. Third, we investigated whether the profile of astrocytic and oligodendrocytic connexins at A/O junctions is altered in Cx32 knockout (KO) mice (Nelles et al., 1996).

MATERIALS AND METHODS

Animals, Antibodies, and Immunoblotting

A total of 25 normal male CD1 mice, 8 male WT C57BL/6 mice, and 9 male C57BL/6 Cx32 KO mice (the latter kindly provided by Dr. K. Willecke, University of Bonn, Germany) were used in this study. The WT and KO C57BL/6 animals were bred according to standard protocols at Colorado State University. Liver and brain from 3 WT and 4 KO mice were taken for western blotting analyses by methods previously described (Li et al., 1997, 1998, 2002; Rash et al., 2001). The remaining mice were used for anatomical studies.

The anti-connexin antibodies used, their sources, and reference citations to previous characterizations are listed in Table 1. Monoclonal and polyclonal anti-Cx32 antibodies directed against different sequences in Cx32 were tested. Antibodies used as markers of oligodendrocytes included monoclonal anti-2, ′3′-cyclic nucleotide 3′-phosphodiesterase (CNPase) (Sternberger Monoclonals, Baltimore, MD), and polyclonal anti-CNPase (Gravel et al., 1994), kindly provided by Dr. P.E. Braun (McGill University, Montreal, Canada).

LM Immunohistochemistry

The mice were deeply anesthetized with equithesin (3 ml/kg) (Scadding, 1981) and perfused transcardially with 3 ml of "prefixative" solution consisting of cold (4°C) 0.1 M sodium phosphate buffer (PB), pH 7.4, containing 0.9% NaCl (PBS), 0.1% sodium nitrite and heparin (1 U/ml). This was followed by perfusion with 20 ml of cold 0.16 M sodium phosphate buffer, pH 7.6, containing 4% formaldehyde and 0.2% picric acid, which was followed by perfusion with 10 ml of PB, pH 7.4, containing 10% sucrose. Brains were removed and stored at 4°C for 48 hr in cryoprotectant consisting of 50 mM PB and 10% sucrose.

Cryostat tissue sections (10 μm thick) were obtained and collected on gelatinized glass slides and processed for immunofluorescence. All antibodies were diluted in 50 mM Tris-HCl, pH 7.4, containing 1.5% NaCl (TBS), 0.3% Triton X-100 (TBST), and 4% normal goat serum (NGS); all washes were carried out in TBST. For single labeling, sections were incubated for 24 h at 4°C with either monoclonal mouse anti-Cx32 (7C7, derived from culture supernatant) diluted 1:25, monoclonal mouse anti-Cx32 (35-8900) diluted 1:400, monoclonal anti-Cx32 (13–8200) diluted 1:500, polyclonal rabbit anti-Cx32 (71–0600) diluted 1:100, or rabbit anti-Cx32 (34–5700) diluted 1:100. After primary antibody incubations, sections were washed for 1 h in TBST and then incubated for 1.5 h at room temperature with either fluorescein isothiocyanate (FITC)-conjugated horse anti-mouse IgG (Vector Laboratories, Burlin-game, CA) diluted 1:100, Cy3-conjugated goat anti-mouse (Jackson ImmunoResearch Laboratories, West Grove, PA) diluted 1:200, or Cy3-conjugated donkey anti-rabbit (Jackson ImmunoResearch) diluted 1:200.

Sections processed for double immunofluorescence labeling of Cx32 and Cx30 were incubated for 24 h at 4°C with monoclonal mouse anti-Cx32 (7C7 or 35–8900) as described above, plus polyclonal rabbit anti-Cx30 (71–2200) diluted 1:100. Alternatively, sections were incubated simultaneously with polyclonal rabbit anti-Cx32 (34–5700) as described above and with monoclonal anti-Cx30 (33–2500) diluted 1:500. Sections were then washed in TBST for 1 hr at room temperature and incubated simultaneously with appropriate combinations of FITC-conjugated horse anti-mouse IgG diluted 1:100, Alexa Fluor-conjugated goat anti-rabbit F(ab′)2 (Molecular Probes, Eugene, OR) diluted 1:1,000, or Cy3-conjugated goat anti-mouse or donkey anti-rabbit IgG (Jackson ImmunoResearch) diluted 1:200. The same protocol was followed for double immunofluorescence labeling of Cx30 and Cx43, using polyclonal rabbit anti-Cx30 diluted 1:100 and monoclonal mouse anti-Cx43 (33-5000) diluted 1:150. Sections were then incubated with appropriate combinations of secondary antibodies, as described above.

Sections processed for double immunofluorescence labeling of CNPase with either Cx26, Cx29, Cx30, Cx32, Cx43, or Cx47 were incubated for 24 h at 4°C with monoclonal mouse anti-CNPase diluted 1:5,000, and simultaneously with either polyclonal rabbit anti-Cx26 (51–2800) diluted 1:200, rabbit anti-Cx29 (34–4200) diluted 1:400, rabbit anti-Cx30, rabbit anti-Cx32 (71–0600 or 34–5700), rabbit anti-Cx43 diluted as above, or rabbit anti-Cx47 (36–4700) diluted 1:400. Additional sections were incubated with polyclonal rabbit anti-CNPase diluted 1:1,000 and simultaneously with either monoclonal mouse anit-Cx26 (33–5800) diluted 1:200, monoclonal anti-Cx32 (7C7 or 35–8900), or monoclonal mouse anti-Cx43 all diluted as above. Sections were then washed and incubated simultaneously with Cy3-conjugated donkey anti-rabbit IgG and FITC-conjugated horse anti-mouse IgG, as described above. All sections were washed for 20 min in TBST, followed by two 20-min washes in 50 mM Tris-HCl buffer, pH 7.4, and coverslipped with antifade medium. Control procedures were conducted by omission of one or the other of the primary antibodies with inclusion of both of the secondary antibodies. No labeling occurred with secondary antibodies that corresponded to the omitted primary antibody.

Fluorescence was examined on a Zeiss Axioskop2 fluorescence microscope and an Olympus Fluoview IX70 confocal microscope. For confocal analysis, double-labeled sections were scanned twice using single laser excitation for one or the other fluorochrome. Images were acquired by single scan of sections at sufficient magnification to discern individual immunolabeled puncta. Images were captured using Axiovision 3.0 (Carl Zeiss Canada, Toronto) software, assembled according to appropriate size and adjusted for contrast based on elimination of "empty" pixels in either Photo-shop 6.0 or Corel Draw 8.

Data Analysis

To determine quantitatively the density of Cx30-positive puncta on the astrocytic side of A/O junctions on oligodendrocyte somata in brains of WT and Cx32 KO mice, the numbers of immunofluorescent puncta on CNPase-positive oligodendrocytes were counted in four different brain regions, including the cerebral cortex, globus pallidus, ventral lateral nucleus of the thalamus, and hypothalamus. Counting was performed under immunofluorescence microscopy at ×40 magnification in a grid-like fashion that allowed examination of consecutively adjacent areas in a nonoverlapping pattern. A conservative approach was taken such that only clearly distinguishable and distinct puncta were counted at a single optimal focal plane on individual oligodendrocyte soma. Data were collected from groups of 3 WT and 3 Cx32 KO mice, and statistically analyzed by Student's *t*-test. The mean number of Cx30-positive puncta (±SEM) surrounding oligodendrocytes in each brain region in each animal was obtained by pooling counts from both sides of the brain for each brain region examined. The total number of oligodendrocytes examined in each brain area in a total of 14 sections from the 3 WT and 3 KO animals is indicated in Table 2. The frequency distribution of the number of Cx30-positive puncta per oligodendrocyte in cortex and globus pallidus was derived by pooling data from three WT animals, and plotted by binning puncta numbers into 12 groups ranging from 0 to 22 puncta.

RESULTS

Cx32 and Cx47 Detection in WT and KO Mice

Five anti-Cx32 antibodies used for immunoblotting of WT mouse liver (and rat liver shown with two of the antibodies for comparison) detected monomeric Cx32 migrating at 30–32 kDa. In contrast no detection of Cx32 was observed in Cx32 KO mice (Fig. 1A). In addition, four of the antibodies detected dimeric Cx32 migrating at 49–52 kDa in normal mouse liver, and this dimer was absent in liver of KO animals. Detection of the dimer form in rat liver was variable. Using two of the anti-Cx32 antibodies, Western blotting of brain tissue revealed Cx32 in the thalamus of WT, but not in the thalamus of Cx32 KO animals (Fig. 1B,C). Dimeric Cx32 was either not detected or was obscured by co-migrating nonspecific bands. Other nonspecific bands are of unknown identity, and possible relationships of these bands to immunofluorescence images are described below. Western blotting of various brain regions from WT mice (Fig. 1D) with anti-Cx47 antibody (directed against a 19-amino acid sequence in the C-terminus of Cx47) showed a band migrating at 50–2 kDa in 9% polyacrylamide gels. Analysis on 12.5% gels gave a similar apparent molecular weight (Fig. 1E), but Cx47 was resolved as a closely migrating doublet of bands, possibly reflecting different posttranslational modification states of Cx47, as has been observed with Cx43 in brain (Li et al., 1998). There were no detectable differences in migration profiles or relative levels of Cx47 in CNS tissues of WT vs Cx32 KO mice (Fig. 1E).

Immunolabeling for Cx32 in liver of WT and Cx32 KO mice is shown in Figure 2A–D. With all five antibodies (data from 13–8200 not shown), nonspecific background immunoreactivity was low and clear punctate labeling was seen around hepatocytes in WT liver, whereas Cx32 labeling was absent in liver of Cx32 KO mice. Similar dense punctate labeling for Cx26 was

evident around hepatocytes in liver of WT mice, but labeling for Cx26 was barely detectable in liver of Cx32 KO animals (not shown), confirming previous reports (Nelles et al., 1996).

LM immunofluorescence was conducted to confirm that Cx32 is expressed by oligodendrocytes in the WT stain of C57BL/6 mice, as reported in other mouse stains (Li et al., 1997; Rash et al., 2001). Double labeling showed that cells immunopositive for the oligodendrocyte marker CNPase (Fig. 2E1) were consistently labeled for Cx32 (Fig. 2E2). Cx32 in brain was also associated with myelin of CNPase-positive fibers (Fig. 2), which accounts for additional Cx32-immunoreactivity not associated with oligodendrocyte somata in fields labeled for Cx32. A similar pattern of labeling around oligodendrocytes was obtained with each of the five anti-Cx32 antibodies. The authenticity of this labeling was tested in Cx32 KO mice. Fields of brain demonstrating the presence of CNPase-positive oligodendrocyte cell bodies and myelinated fibers (Fig. 2F1) exhibited total absence of labeling of somata and myelinated fibers (Fig. 2F2) with all five Cx32 antibodies. In WT mice, widespread Cx32 labeling of oligodendrocyte somata is illustrated in a field of hypothalamus (Fig. 2G1). In KO mice, the absence of Cx32 labeling is illustrated in similar areas of hypothalamus (Fig. 2G2).

Despite the occasional presence of nonspecific bands observed on Western blots of brain tissue with some anti-Cx32 antibodies, all Cx32 immunolabeling was absent in brain of Cx32 KO mice with antibodies 7C7, 35–8900 and 34–5700. However, in addition to labeling of oligodendrocytes, antibody 13–8200 gave intense, diffuse labeling throughout brain, and antibody 71–0600 labeled fine varicose axons in restricted brain regions (e.g., amygdala), neither of which was eliminated in Cx32 KO animals, indicating cross-reactions with other proteins. Thus, the use of the latter two antibodies for immunohistochemical studies involving CNS tissues requires caution. In addition, a difficulty was encountered with monoclonal anti-Cx30 (33–2500). While single immunolabeling with this antibody produced robust detection of Cx30 in brain, double labeling with accompanying controls revealed that monoclonal anti-Cx30 not only was detected by anti-mouse secondary antibodies, but also by Cy3-, FITC- and Al-exaFuor-conjugated anti-rabbit antibodies (Jackson ImmunoResearch Laboratories; Molecular Probes). This cross-species reactivity precludes use of Ab33-2500 for double labeling with rabbit primary antibodies.

Connexin Localization in WT Mice

Laser scanning confocal immunofluorescence, undertaken to confirm Cx32 localization to oligodendrocytes in C57BL/C6 mice, demonstrated numerous Cx32-positive puncta around oligodendrocyte cell bodies and their initial processes (Fig. 3A). A similar pattern of labeling around oligodendrocytes was obtained with each of the five anti-Cx32 antibodies, four of which were used in subsequent confocal LM studies, with the exclusion of 13–8200.

To establish widespread astrocytic Cx30 association with oligodendrocytic Cx32 by LM, as reported in restricted brain regions examined by EM (Rash et al., 2001), confocal analysis was conducted after double labeling for these two connexins in brain sections from WT C57BL/6 mice. In cerebral cortex, Cx30 labeling was widespread, primarily reflecting the distribution of A/A gap junctions. However, a small fraction of Cx30-positive puncta overlapped with Cx32-positive puncta (Fig. 3B) in a manner reflecting the distribution pattern of Cx32 associated with CNPase (Fig. 3A). Similar results were obtained in many brain regions examined including globus pallidus (Fig. 3C), ventrolateral thalamic nucleus (Fig. 3D), and ventroanterior thalamus nucleus (Fig. 3E), where only the overlays of double labeling for Cx30 and Cx32 are shown. In fields labeled for Cx32, immunoreactivity not localized to oligodendrocyte somata was associated with CNPase-positive myelinated fibers (Fig. 3A). Double labeling for Cx43 and Cx30 also showed co-localization of these two connexins on the surface of oligodendrocytes (Fig. 3F), consistent with previous demonstrations of Cx43

association with Cx32 on these cells (Rash et al., 2001). Similar results were obtained in brain sections of CD1 mice (not shown).

Connexin Localization in Cx32 KO Mice

The deployment of astrocytic Cx30, Cx43, and Cx26 to the surface of oligodendrocytes was examined in Cx32 KO and compared with their distributions in WT mice. In cerebral cortex and many subcortical regions of WT brain, oligodendrocytes were conspicuous in sections labeled for Cx30 by virtue of their dense decoration with Cx30-positive puncta (Fig. 4A).

Immunofluorescence of oligodendrocyte-associated Cx30 puncta was usually more intense than the more widely distributed Cx30 puncta that presumably were localized to gap junctions between astrocytes (Nagy et al., 1999, 2001; Rash et al., 2001). In similar fields of cerebral cortex and other regions of Cx32 KO brain, oligodendrocytes were virtually devoid of Cx30-positive puncta (Fig. 4B). Confocal analysis of cerebral cortex confirmed that CNPase-positive cells in cerebral cortex of WT mice were decorated by Cx30-positive puncta (Fig. 4C), while CNPase-positive cells in cerebral cortex of Cx32 KO mice displayed vastly reduced labeling for Cx30 (Fig. 4G). Similar results were obtained in other brain regions of WT and Cx32 KO mice including globus pallidus (Fig. 4D,H), ventrolateral thalamic nucleus (Fig. 4E,I), and hypothalamus (Fig. 4F,J).

Frequency distributions of the percentage of CNPase-positive oligodendrocytes displaying puncta on their surface at a single focal plane in fields of cerebral cortex and globus pallidus is shown in Figure 5. The data shown are an underestimate of the number of puncta per oligodendrocyte, as out-of-focus puncta on cells were not counted. Nevertheless, these images indicate that oligodendrocytes displayed a wide range of Cx30 puncta, with most oligodendrocyte images having seven to eight puncta in a single focal plane. In four brain areas examined quantitatively and within the limit of LM resolution, Cx30-labeled puncta on CNPase-positive oligodendrocytes were reduced by 90% in Cx32 KO compared with WT mice (Table 2).

The density and distribution of Cx43-positive puncta on CNPase-positive oligodendrocytes in cerebral cortex of WT mice (Fig. 6A) were similar to those in Cx32 KO mice (Fig. 6E). Although not quantified, similar results were obtained in other brain areas, including striatum, globus pallidus, and ventroanterior thalamic nucleus, as shown by overlay of double-labeled images of these areas of WT (Fig. 6B–D) and KO (Fig. 6F–H) animals. The distribution of Cx47 around CNPase-positive oligodendrocyte somata and their initial processes throughout CNS of WT mice was very similar to that of Cx32 in cerebral cortex (Fig. 6I) and other brain regions examined (Fig. 6J–L). Preliminary FRIL and thin-section EM results indicate Cx47 localization on the oligodendrocyte side of gap junctions that these cells form with astrocytes (unpublished observations). In Cx32 KO mice, no change in the distribution of Cx47-positive puncta around oligodendrocytes was evident in cerebral cortex (Fig. 6M) or other brain areas (Fig. 6N–P).

Analysis of double labeling for CNPase and Cx26 in various subcortical brain areas revealed oligodendrocytes displaying numerous Cx26-positive puncta on their surface in WT mice (Fig. 7A), with patterns similar to that of Cx30 and Cx43, whereas CNPase-positive cells exhibited reduced Cx26-positive puncta in Cx32 KO mice (Fig. 7B). Although not quantitatively analyzed, this result was representative of hundreds of CNPase-positive oligodendrocytes examined in five WT and five KO mice. The expression and localization of Cx29 in oligodendrocytes (described in detail elsewhere, Nagy et al., 2003a) was dissimilar to the appearance of labeling for Cx32 and Cx47 associated with oligodendrocytes in that Cx29 immunofluorescence appeared as much finer puncta localized to the somatic plasma membrane, with some labeling evident intra-cellularly, and was rarely observed on initial

processes in adult animals. No differences in Cx29 immunoreactivity around oligodendrocytes were evident from comparisons of CNPase/Cx29 double labeling in brains of WT (Fig. 7C) and Cx32 KO (Fig. 7D) animals.

DISCUSSION

The present results demonstrate that several of the anti-Cx32 antibodies used immunohistochemically (7C7, 35–8900, 34–5700) detect exclusively Cx32 in the CNS, whereas other antibodies have additional cross-reactivities (13–8200, 71–0600). Three of the antibodies produced labeling associated with oligodendrocytes in WT mice, and no residual labeling associated with glia or neurons was seen in Cx32 KO mice. Cx30 was shown to be heavily distributed around oligodendrocyte somata, where it was invariably co-localized with astrocytic Cx43 and co-associated with oligodendrocytic Cx32. Comparisons of astrocytic connexins at the surface of oligodendrocytes in WT and Cx32 KO mice indicated that Cx26 and Cx30 were reduced, while Cx43 appeared to be unaffected. Deletion of Cx32 had little effect on Cx29 and Cx47 in oligodendrocytes. These results were consistently obtained after examination of hundreds of oligodendrocytes in dozens of brain sections from over thirty animals subjected to various fixation conditions.

Our findings may be viewed in light of knowledge concerning compatibility of connexin coupling partners. Following identification of Cx43 expression in astrocytes (Dermietzel et al., 1989; Yamamoto et al., 1990a,b) and Cx32 expression in oligodendrocytes (Scherer et al., 1995; Dermietzel et al., 1997; Kunzelmann et al., 1997; Li et al., 1997), the nature of gap junction channels between these two cell types remained uncertain because Cx43 and Cx32 were found to be nonpermissive for forming functional GJIC channels (Swenson et al., 1989; Werner et al., 1989; Elfgang et al., 1995). This raised the possibility that these macroglial cells express other connexins. This conjecture was confirmed with the identification of Cx30 in astrocytes (Nagy et al., 1997, 1999; Kunzelmann et al., 1999), allowing for permissive coupling of oligodendrocytic Cx32 with astrocytic Cx30 (Dahl et al., 1996). However, the participation of yet other connexins in A/O gap junctions remained likely in view of observations that while gap junctions and GJIC occur between astrocytes and oligodendrocytes in gray matter (Mugnaini, 1986; Rash et al., 1997; Pastor et al., 1998), Cx30 is not present in white matter astrocytes (Nagy et al., 1999), leaving Cx32 in white matter oligodendrocytes with an unidentified astrocytic connexin coupling partner. This difficulty was potentially overcome by recent reports of Cx26 expression by astrocytes and localization of Cx26 on the astrocyte side of A/O gap junctions (Mercier and Hatton, 2001; Nagy et al., 2001), together with compatibility of functional Cx26/Cx32 junction formation (White and Bruzzone, 1996). Still other combinations of coupling at these junctions were likely, as oligodendrocytes in brain have recently been found to express Cx29 and Cx47 (Altevogt et al., 2002; Nagy et al., 2003a,b). Oligodendrocytes have also been reported to express Cx45 (Kunzelmann et al., 1997; Dermietzel et al., 1997). Although highly expressed in sciatic nerve (Altevogt et al., 2002; Li et al., 2002), Cx29 was sparse on oligodendrocyte somata, exhibited limited co-localization with Cx32 on these cells, and failed to display the pattern of punctate labeling characteristic of astrocytic Cx30 and Cx43 abutments on oligodendrocytes (Nagy et al., 2003a). Consequently, Cx29 is unlikely to play a major role in the formation of intercellular A/O gap junctions.

In heterologous gap junctions between cells expressing multiple connexins and having the capability of forming various combinations of heterotypic connexon channels, it is not evident a priori that a particular connexin, among several others on one side of a plaque, will fail to be incorporated into the plaque if its sole coupling partner, among several connexins on the other side, is absent. Gap junctions between astrocytes and oligodendrocytes provide a rare opportunity to address this issue in vivo because this is a heterologous coupling situation in

which the three connexins on one side differ completely from those on the other side, allowing eventual analysis of how each connexin deletion on one side of a junction affects the connexins on the other side. At A/O gap junctions in adult Cx32 KO mice, the present results indicate that Cx30 is vastly or completely reduced, and that Cx26 is partially reduced on the astrocyte side after elimination of Cx32 on the oligodendrocyte side, whereas astrocytic Cx43 and oligodendrocytic Cx29 and Cx47 appear unaffected. Thus, it may be speculated that the stability of particular connexins at A/O gap junctions requires specifically the presence of its coupling partner. Thus, we infer that at A/O junctions, Cx32 couples extensively or exclusively with Cx30, but may couple to a limited extent with Cx26. Conversely, the presence of a small amount of Cx26 immunoreactivity on the astrocyte side of A/O junctions in Cx32 KO mice may suggest that Cx26 couples to an additional connexin in oligodendrocytes, presumably Cx47 and perhaps minimally with Cx29 given the low levels of this connexin on oligodendrocyte somata in adult brain. The maintained presence of Cx43 on the astrocyte side of A/O junctions in Cx32 KO mice suggests that Cx43 does not couple with Cx32, consistent with the nonpermissiveness of this combination (White and Bruzzone, 1996). Rather, Cx43 is presumed to couple with Cx47. The organization of gap junction channels within individual junctional plaques containing two or more different connexins on each side becomes potentially more complicated given the existence of heteromeric connexons (Brink et al., 1997; Diez et al., 1999) consisting of various proportions of different connexins. This complicating factor is supported by observations that coupling of heteromeric connexons may alter permselectivities (Bevans et al., 1998).

The widespread occurrence of A/O gap junctions in the CNS is consistent with reports describing gap junction-mediated electrical and/or dye-coupling between astrocytes and oligodendrocytes both in vivo and in vitro (Ransom and Kettenmann, 1990; Robinson et al., 1993; Venance et al., 1995). However, reports that gap junctions between oligodendrocytes occur rarely if ever in brain and spinal cord (Mugnaini, 1986; Rash et al., 1997 Rash et al., 2000) are difficult to reconcile with observations of dye-coupling between these cells in spinal cord and optic nerve, as well as in cell culture (Kettenmann and Ransom, 1988; Kettenmann et al., 1990; Ransom and Kettenmann, 1990; Von Blankenfeld et al., 1993; Butt and Ransom, 1993; Venance et al., 1995; Takeda et al., 1995; Pastor et al., 1998). It may be that different patterns of connexin expression and junctional coupling occur between oligodendrocytes in different CNS regions, which also could be reflected in vitro. Although there is little evidence for this as yet, this possibility remains to be more fully explored. Alternatively, some of the coupling observed between these cells may be mediated by astrocyte intermediaries, e.g., O/A/O, as previously proposed (Mugnaini, 1986; Rash et al., 2001). In this event, coupling observed between oligodendrocytes in gray matter but not white matter in spinal cord (Pastor et al., 1998) may result in part from Cx30 expression in gray but not white matter astrocytes, and hence the absence of this connexin on the astrocyte side of A/O gap junctions in white matter (Nagy et al., 1999). Finally, the completely different set of connexins expressed in astrocytes compared to those in oligodendrocytes, which requires that A/O gap junctions be entirely heterotypic, may provide the basis for the reported unidirectional dye movement from astrocyte to oligodendrocyte, but not from oligodendrocyte to astrocyte at retinal A/O gap junctions (Robinson et al., 1993). The mechanism for such unidirectional coupling would be difficult to imagine were these junctions to contain a homotypic connexin coupling component.

The influence of Cx32 deletion on connexin coupling between glial cells is relevant to considerations of X-linked Charcot-Marie-Tooth disease, in which Cx32 mutations result in peripheral neuropathy and in CNS alterations (Bergoffen, 1993; Bone et al., 1997; Bahr et al., 1999; Panas et al., 1998). Although it remains unclear whether other glial connexins are able to compensate for functional loss of Cx32, our findings suggest that the high levels of Cx43/Cx47 may provide a mechanism for compensation. Conversely, the low levels of Cx29 on oligodendrocyte somata in both WT and Cx32 KO mice suggest that little compensation may

occur through pairing of oligodendrocyte Cx29 with astrocytic Cx26, Cx30, or Cx43. These results also indicate that cellular trafficking and targeting of Cx29 and Cx47 are essentially independent of Cx32 expression, although possible deleterious actions of mutated Cx32 on processing of these other two oligodendrocytic connexin remain to be investigated. It also remains to be determined whether Cx32 mutations impact on localization and function of Cx29 and Cx32 in regions of uncompacted, internodal CNS myelin, which contain an abundance of these connexins (Altevogt et al., 2002; Nagy et al., 2003a). Consideration of connexin compensation must also take into account the wide range in permselectivity of junctional channels formed by various connexin combinations (Veenstra, 1996). In gap junctions between cells expressing several connexins, the presence of junctions formed by the remaining connexin pairs after deletion of one connexin may not represent compensation because the deleted connexin may mediate passage of different substances than the remaining connexins. The developmental stage of connexin expression is an additional factor to consider. It has been reported, for example, that onset of Cx30 expression in brain occurs relatively late during development (Nagy et al., 1999; Kunzelmann et al., 1999), with Cx30 protein expression at post-natal day 20 in mice being minimal as compared with that seen in adult brain (Nagy et al., 1999). Thus, any deficits in function due to reduced pairing of Cx30/Cx32 at A/O junctions in Cx32 KO mice may not be evident until after CNS development is largely complete, and any damage resulting from (or compensation of) function by other connexins may not be occur until a similar late developmental stage.

Acknowledgements

This work was supported by grants from the CIHR (to J.I.N.), and by NIH grant NS-31027, NS-44010 and NS-44395 (to J.E.R.). The authors thank B. McLean, C. Olson, and N. Nolette for assistance; Dr. K. Willecke for Cx32 KO mice; and Dr. P.E. Braun for providing anti-CNPase.

References

Altevogt BM, Kleopa KA, Postma FR, Scherer SS, Paul DL. Connexin29 is uniquely distributed within myelinating glial cells of the central and peripheral nervous systems. J Neurosci 2002;22:6458–6470. [PubMed: 12151525]

Bahr M, Andres F, Timmerman V, Nelis ME, Van Broeckhoven C, Dichgans J. Central visual, acoustic and motor pathway involvement in Charcot-Marie-Tooth family with an asn205ser mutation in the connexin32 gene. J Neurol Neurosurg Psychiatry 1999;66:202–206. [PubMed: 10071100]

Bergoffen J, Scherer SS, Wang S, Oronzi-Scott M, Bone L, Paul DL, Chen K, Lensch MW, Chance P, Fischbeck K. Connexin mutations in X-linked Charcot-Marie-Tooth disease. Science 1993;262:2039–2042. [PubMed: 8266101]

Bevans CG, Kordel M, Rhee SK, Harris AL. Isoform composition of connexin channels determines selectivity among second messengers and uncharged molecules. J Biol Chem 1998;273:2808–2816. [PubMed: 9446589]

Bone LJ, Deschênes SM, Balice-Gordon RJ, Fischbeck KH, Scherer SS. Connexin 32 and X-linked Charcot-Marie-Tooth disease. Neurobiol Dis 1997;4:221–230. [PubMed: 9361298]

Brink PR, Cronin K, Banach K, Peterson E, Westphale EM, Seul KH, Ramanan SV, Beyer EC. Evidence for heteromeric gap junction channels formed from rat connexin43 and connexin37. Am Physiol Soc 1997;273:C1386–C1396.

Butt AM, Ransom BR. Morphology of astrocytes and oligodendrocytes during development in the intact optic nerve. J Comp Neurol 1993;338:141–158. [PubMed: 8300897]

Dahl E, Manthey D, Chen Y, Schwarz H-J, Chang S, Lalley PA, Nicholson BJ, Willecke K. Molecular cloning and functional expression of mouse connexin30, a gap junction gene highly expressed in adult brain and skin. J Biol Chem 1996;271:17903–17910. [PubMed: 8663509]

Dermietzel R, Traub O, Hwang TK, Beyer E, Bennett MVL, Spray DC, Willecke K. Differential expression of three gap junction proteins in developing and mature brain tissues. Proc Natl Acad Sci USA 1989;86:10148–10152. [PubMed: 2557621]

Dermietzel R, Farooq M, Kessler JA, Hertzberg EL, Spray DC. Oligodendrocytes express gap junction proteins connexin32 and connexin45. Glia 1997;20:101–114. [PubMed: 9179595]

Diez JA, Ahmad S, Evans WH. Assembly of heteromeric connexons in guinea-pig liver en route to the Golgi apparatus, plasma membrane and gap junction. Eur J Biochem 1999;262:142–148. [PubMed: 10231375]

Elfgang C, Eckert R, Lichtenberg-Frate H, Butterweck A, Traub O, Klein RA, Hulser DF, Willecke K. Specific permeability and selective formation of gap junction channels in connexin-transfected HeLa cells. J Cell Biol 1995;129:805–817. [PubMed: 7537274]

Gravel M, DeAngelis D, Braun PE. Molecular cloning and characterization of rat brain 2′,3′-cyclic nucleotide 3′-phosphodies-terase isoform 2. J Neurosci Res 1994;15:243–247. [PubMed: 7932861]

Kettenmann H, Ransom BR. Electrical coupling between astrocytes and between oligodendrocytes studied in mammalian cell cultures. Glia 1988;1:64–73. [PubMed: 2853139]

Kettenmann H, Ransom BR, Schlue W-R. Intracellular pH shifts capable of uncoupling cultured oligodendrocytes are seen only in low HCO_3 solution. Glia 1990;3:110–117. [PubMed: 2139632]

Kunzelmann P, Blumcke I, Traub O, Dermietzel R, Willecke K. Coexpression of connexin45 and -32 in oligodendrocytes of rat brain. J Neurocytol 1997;26:17–22. [PubMed: 9154525]

Kunzelmann P, Schröder W, Traub O, Steinhä user C, Dermietzel R, Willecke K. Late onset and increasing expression of the gap junction protein connexin30 in adult murine brain and long-term cultured astrocytes. Glia 1999;25:111–119. [PubMed: 9890626]

Li J, Hertzberg EL, Nagy JI. Connexin32 in oligodendrocytes and association with myelinated fibers in mouse and rat brain. J Comp Neurol 1997;379:571–591. [PubMed: 9067844]

Li WEI, Ochalski PAY, Hertzberg EL, Nagy JI. Immunorecognition, ultrastructure and phosphorylation status of astrocytic gap junctions and connexin43 in rat brain after cerebral focal ischemia. Eur J Neurosci 1998;10:2444–2463. [PubMed: 9749772]

Li, Xinbo; Lynn, BD.; Olson, C.; Meier, C.; Davidson, KGV.; Yasumura, T.; Rash, JE.; Nagy, JI. Connexin29 expression, immunocytochemistry and freeze-fracture replica immunogold labeling (FRIL) in sciatic nerve. Eur J Neurosci 2002;16:795–806. [PubMed: 12372015]

Mercier F, Hatton GI. Connexin 26 and basic fibroblast growth factor are expressed primarily in the subpial and subependymal layers in adult brain parenchyma: roles in stem cell proliferation and morphological plasticity? J Comp Neurol 2001;431:88–104. [PubMed: 11169992]

Mugnaini, E. Cell junctions of astrocytes, ependyma, and related cells in the mammalian central nervous system, with emphasis on the hypothesis of a generalized functional syncytium of supporting cells. In: Fedoroff, S.; Vernadakis, A., editors. Astrocytes. I. San Diego, CA: Academic Press; 1986. p. 329-371.

Nagy JI, Ochalski PAY, Li J, Hertzberg EL. Evidence for co-localization of another connexin with connexin-43 at astrocytic gap junctions in rat brain. Neuroscience 1997;78:533–548. [PubMed: 9145808]

Nagy JI, Patel D, Ochalski PAY, Stelmack GL. Connexin30 in rodent, cat and human brain: selective expression in gray matter astrocytes, co-localization with connexin30 at gap junctions and late developmental appearance. Neuroscience 1999;88:447–468. [PubMed: 10197766]

Nagy JI, Li X, Rempel J, Stelmack G, Patel D, Staines WA, Yasumura T, Rash JE. Connexin26 in adult rodent CNS: demonstration at astrocytic gap junctions and co-localization with connexin30 and connexin43. J Comp Neurol 2001;441:302–323. [PubMed: 11745652]

Nagy JI, Ionescu AV, Lynn BD, Rash JE. Connexin29 and connexin32 at oligodendrocyte/astrocyte gap junctions and in myelin of mouse CNS. J Comp Neurol. 2003ain press

Nagy JI, Dudek FE, Rash JE. Update on connexins and gap junctions in neurons and glia in the nervous system. Brain Res Rev. 2003bin press

Nelles E, Butzler C, Jung D, Temme A, Gabriel H-D, Dahl U, Traub O, Stumpel F, Jungermann K, Zielasek J, Toyka KV, Dermietzel R, Willecke K. Defective propagation of signals generated by sympathetic nerve stimulation in the liver of connexin32-deficient mice. Proc Natl Acad Sci USA 1996;93:9565–9570. [PubMed: 8790370]

Panas M, Karadimas C, Avramopoulos D, Vassilopoulos D. Central nervous system involvement in four patients with Charcot-Marie-Tooth disease with connexin32 extracellular mutations. J Neurol Neurosurg Psychiatry 1998;65:947–948. [PubMed: 9854984]

Pastor A, Kremer M, Möller T, Kettenmann H, Dermietzel R. Dye coupling between spinal cord oligodendrocytes: differences in coupling efficiency between gray and white matter. Glia 1998;24:108–120. [PubMed: 9700494]

Ransom BR, Kettenmann H. Electrical coupling, without dye coupling, between mammalian astrocytes and oligodendrocytes in cell culture. Glia 1990;3:258–266. [PubMed: 2144505]

Rash JE, Duffy HS, Dudek FE, Bilhartz BL, Whalen LR, Yasumura T. Grid-mapped freeze-fracture analysis of gap junctions in gray and white matter of adult rat central nervous system, with evidence for a "panglial syncytium" that is not coupled to neurons. J Comp Neurol 1997;388:265–292. [PubMed: 9368841]

Rash JE, Yasumura T, Dudek FE, Nagy JI. Cell-specific expression of connexins and evidence of restricted gap junctional coupling between glial cells and between neurons. J Neurosci 2001;21:1983–2000. [PubMed: 11245683]

Robinson SR, Hampson ECGM, Munro MN, Vaney DI. Unidirectional coupling of gap junctions between neuroglia. Science 1993;262:1072–1074. [PubMed: 8093125]

Scadding JW. Development of ongoing activity, mechanosensitivity, and adrenaline sensitivity in severed peripheral nerve axons. Exp Neurol 1981;73:345–364. [PubMed: 7262242]

Scherer SS, Deschenes SM, Xu Y-T, Grinspan JB, Fischbeck KH, Paul DL. Connexin32 is a myelin-related protein in the PNS and CNS. J Neurosci 1995;15:8281–8294. [PubMed: 8613761]

Swenson KI, Jordan JR, Beyer EC, Paul DL. Formation of gap junctions by expression of connexins in *Xenopus* oocyte pairs. Cell 1989;57:145–155. [PubMed: 2467743]

Takeda M, Nelson DJ, Soliven B. Calcium signaling in cultured rat oligodendrocytes. Glia 1995;14:225–236. [PubMed: 7591034]

Veenstra RD. Size and selectivity of gap junction channels formed from different connexins. J Bioenerg Biomembr 1996;28:327–337. [PubMed: 8844330]

Venance L, Cordier J, Monge M, Zalc B, Glowinski J, Giaume C. Homotypic and heterotypic coupling mediated by gap junctions during glial cell differentiation in vitro. Eur J Neurosci 1995;7:451–461. [PubMed: 7773442]

Von Blankenfeld G, Ransom BR, Kettenmann H. Development of cell-cell coupling among cells of the oligodendrocyte lineage. Glia 1993;7:322–328. [PubMed: 8320002]

Werner RE, Levine C, Rabadan-Diehl C, Dahl G. Formation of hybrid channels. Proc Natl Acad Sci USA 1989;86:5380–5384. [PubMed: 2546155]

White TW, Bruzzone R. Multiple connexin proteins in single intercellular channels: connexin compatibility and functional consequences. J Bioenerg Biomembr 1996;28:339–349. [PubMed: 8844331]

Willecke K, Eiberger J, Degen J, Eckardt D, Romualdi A, Guldenagel M, Deutsch U, Sohl G. Structural and functional diversity of connexin genes in the mouse and human genome. Biol Chem 2002;383:725–737. [PubMed: 12108537]

Wolburg H, Rohlmann A. Structure-function relationships in gap junctions. Int Rev Cytol 1995;157:315–373. [PubMed: 7706021]

Yamamoto T, Ochalski PAY, Hertzberg EL, Nagy JI. LM and EM immunolocalization of the gap junctions protein connexin43 in rat brain. Brain Res 1990a;508:313–319. [PubMed: 2155040]

Yamamoto T, Ochalski PAY, Hertzberg EL, Nagy JI. On the organization of astrocytic gap junctions in rat brain as suggested by LM and EM immunohistochemistry of connexin43 expression. J Comp Neurol 1990b;302:853–883. [PubMed: 1964467]

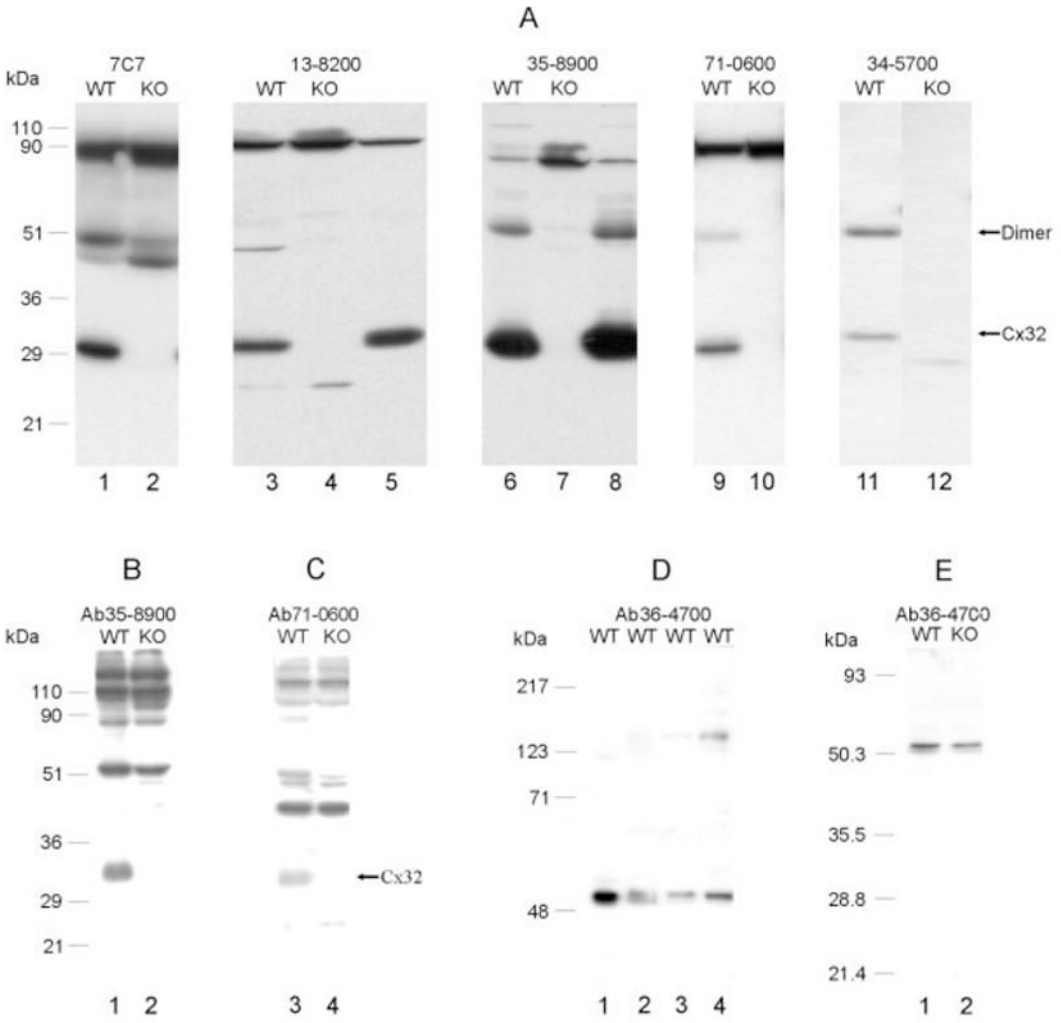

Fig. 1.

A: Western blots of liver from wild-type (WT) and Cx32 knockout (KO) mice probed with five different anti-Cx32 antibodies listed in Table 1 and indicated above each blot. Monomeric Cx32 is detected migrating at about 30–32 kDa in liver from WT mice (**lanes 1, 3, 6, 9, 11**), but is absent in liver of Cx32 KO mice (**lanes 2, 4, 7, 10, 12**). Detection of Cx32 in rat liver with two of the antibodies is shown for comparison (lanes 5, 8). Four of the antibodies detect a dimeric Cx32 in WT mice (**lanes 3, 6, 9, 11**), which is also absent in Cx32 KO mice (**lanes 4, 7, 10, 12**). Some nonspecific bands are evident, particularly with antibody 7C7, where detection of dimeric Cx32 is obscured by reaction with a similarly migrating protein. **B,C**: Western blots of brain homogenate from WT and Cx32 KO mice probed with anti-Cx32 antibodies indicated above each blot. Both antibodies detect Cx32 in brain of WT mice and show its absence in Cx32 KO mice. The higher molecular weight bands recognized are of unknown identity. **D**: Western blots of various CNS regions (thalamus, **lane 1**; spinal cord, **lane 2**; hypothalamus, **lane 3**; cerebellum, **lane 4**) (9% gels) probed with anti-Cx47 antibody 36–4700 show Cx47 migrating at about 50–52 kDa. **E**: A doublet of bands is recognized by anti-Cx47 antibody after separation of spinal cord protein on 12.5% gels, with no apparent difference in levels or migration profile in tissue from WT compared with Cx32 KO mice.

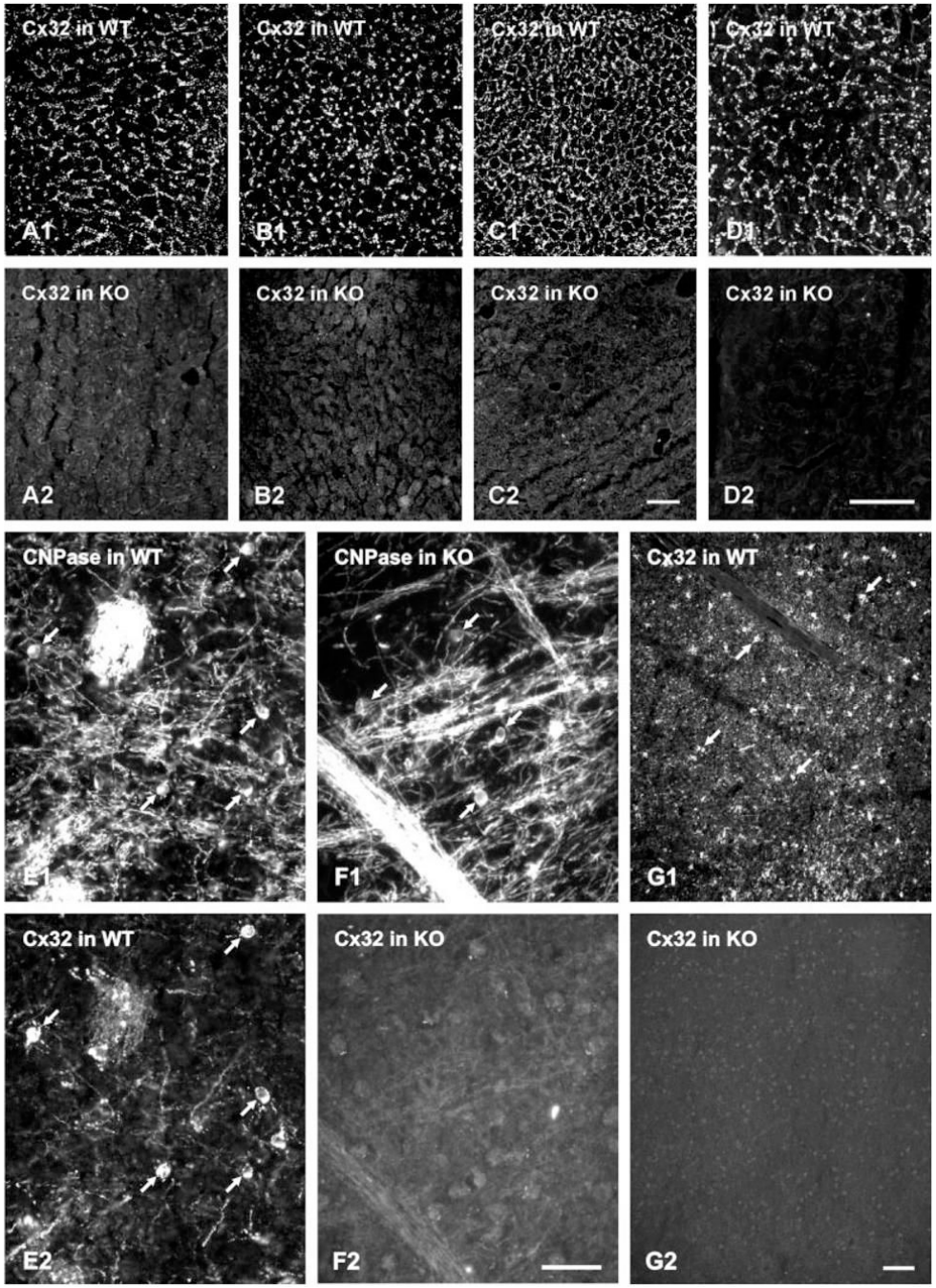

Fig. 2.

A–D: Immunofluorescence labeling for Cx32 with various antibodies in liver of wild-type (WT) and Cx32 knockout (KO) mice. A,B, 7C7; C,D, 71-0600. E,F, 34-5700; G,H, 35-8900. With each antibody, punctate labeling is seen around hepatocytes in liver of Cx32 WT mice, and a total absence of labeling is seen in liver of Cx32 KO mice. **E**: Immunofluorescence double labeling in hypothalamus from a WT mouse showing oligodendrocyte cell bodies immunopositive for both CNPase (E1, arrows) and Cx32 (E2, arrows). **F**: A field in globus pallidus of a Cx32 KO mouse labeled for CNPase to identify oligodendrocytes (F1, arrows), and the same field labeled for Cx32 showing total absence of immunoreactivity (F2). **G**: Low-magnification micrographs showing more than 60 oligodendrocyte cell bodies labeled for Cx32

in hypothalamus of a WT mouse (G1, arrows), and a similar area in hypothalamus of a Cx32 KO mouse showing a total absence of labeling for Cx32 (F). Scale bars = 20 μm in A–C; 40 μm in D–G.

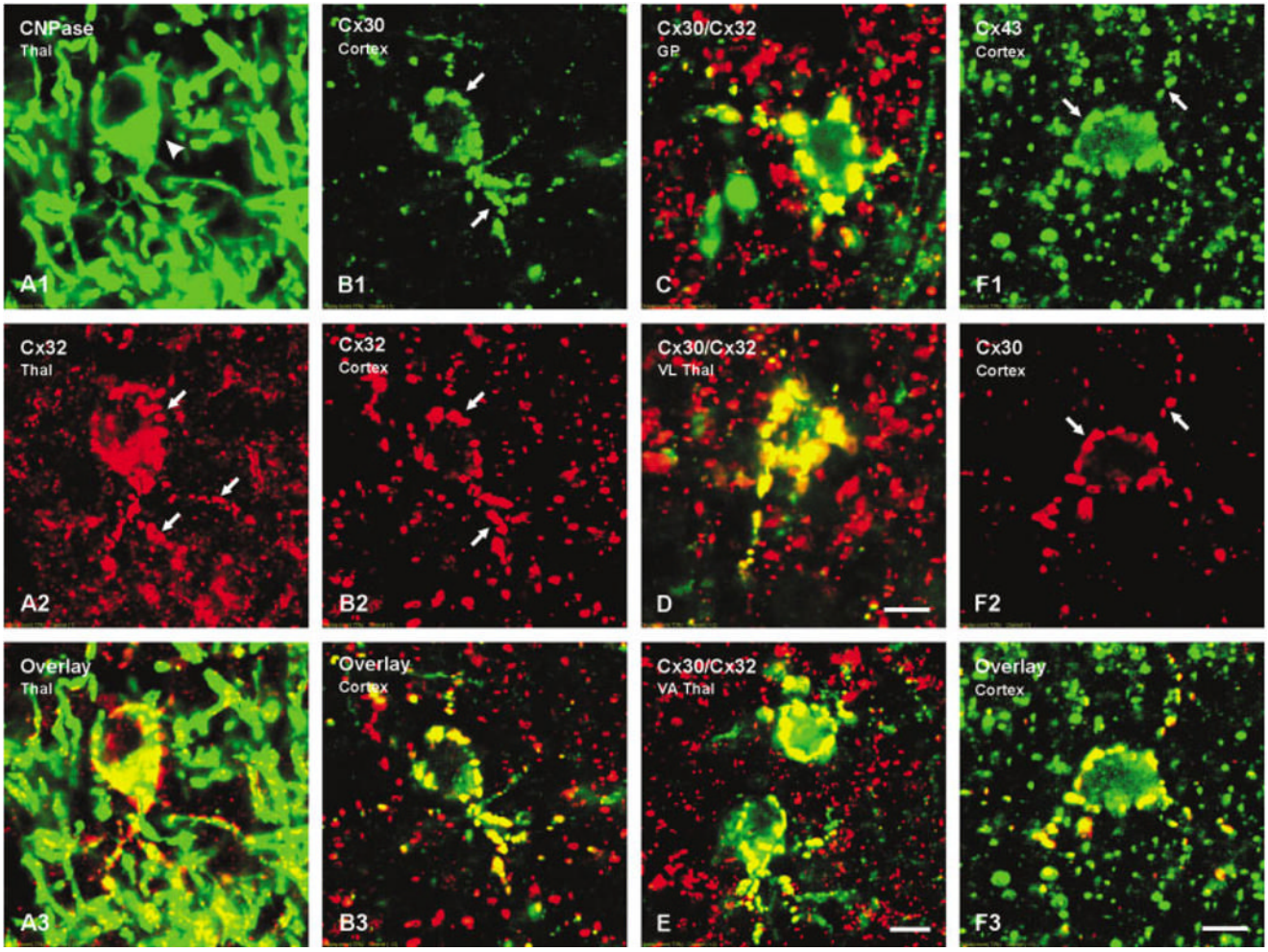

Fig. 3.

Laser scanning confocal immunofluorescence of connexin association with oligodendrocytes in various brain regions of wild-type (WT) mice. **A**: Confocal double labeling in an area of the thalamus showing a CNPase-immunopositive oligodendrocyte (A1, arrowhead) with numerous Cx32-immunopositive puncta (A2, arrows) on the cell body and initial processes (yellow in overlay image, A3). **B**: Confocal double labeling in the cerebral cortex showing Cx30-immu-nopositive puncta (B1, arrows) co-associated with Cx32-immunopositive puncta (B2, arrows) on an oligodendrocyte (yellow in overlay image, B3). **C–E**: Confocal micrographs showing Cx30 (green) co-association with Cx32 (red) as seen by yellow in overlay images from globus pallidus (C), ventrolateral thalamic nucleus (D) and ventroanterior thalamic nucleus (E). F: Double labeling in cerebral cortex showing Cx43-immunopositive puncta (F1, arrows) co-localized with Cx30-immunopositve puncta (F2, arrows) on an oligodendrocyte (yellow in overlay image, F3). Scale bars = 5 μm.

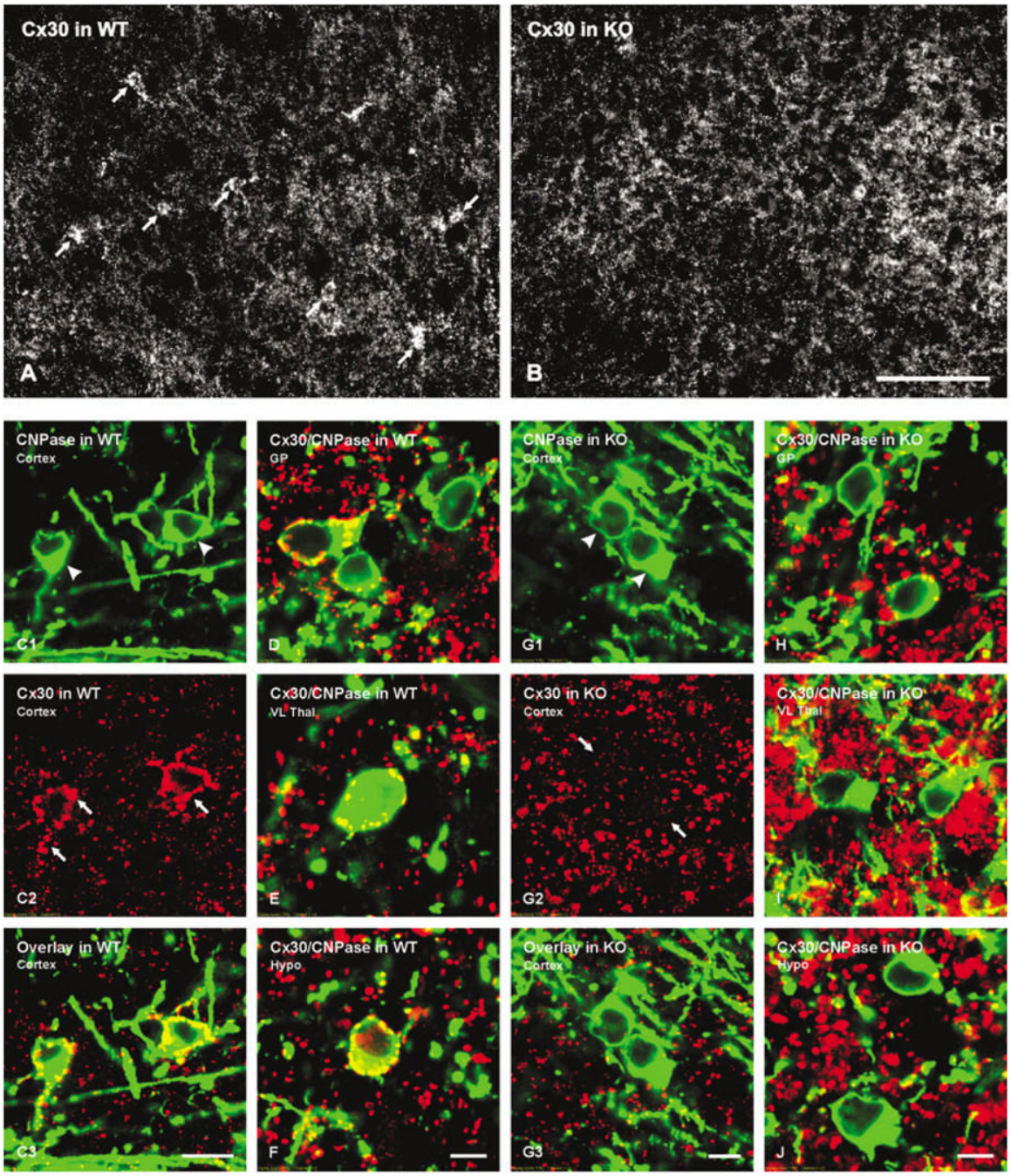

Fig. 4.

Immunofluorescence micrographs showing Cx30 in brains of wild-type (WT) and Cx32 knockout (KO) mice. **A,B**: A field in cerebral cortex of a WT mouse showing oligodendrocytes (A, arrows) densely surrounded by punctate labeling for Cx30, and a similar field in cortex of a Cx32 KO mouse showing absence of labeling for Cx30 on oligodendrocytes (B). Cx30-immunopositive puncta that are not associated with oligodendrocytes appear similar in WT and Cx32 KO mice. **C–J**: Laser scanning confocal immunofluorescence of Cx30 association with oligodendrocytes in various brain regions of WT and Cx32 KO mice. C: Confocal double labeling in cerebral cortex of WT mouse showing two CNPase-positive oligodendrocytes (C1, arrowheads) each decorated with Cx30-positive puncta (C2, arrows) indicated by yellow in

overlay image (C3). D–F: Confocal micrographs from WT mouse showing CNPase (green) co-association with Cx30 (red), as seen by yellow in overlay images from globus pallidus (D), ventrolateral thalamic nucleus (E) and hypothalamus (F). G: Confocal double labeling in cerebral cortex of Cx32 KO mouse showing two CNPase-positive oligodendrocytes (G1, arrowheads) both lacking Cx30-positive puncta (G2, arrows) on their surfaces, as seen by absence of yellow in the overlay image (E3). H–J: Confocal micrographs from Cx32 KO mouse showing lack of CNPase (green) and Cx30 (red) co-association in globus pallidus (H), ventrolateral thalamic nucleus (I) and hypothalamus (J). Scale bars = 40 μm in A,B; 10 μm in C; 5 μm in D–J.

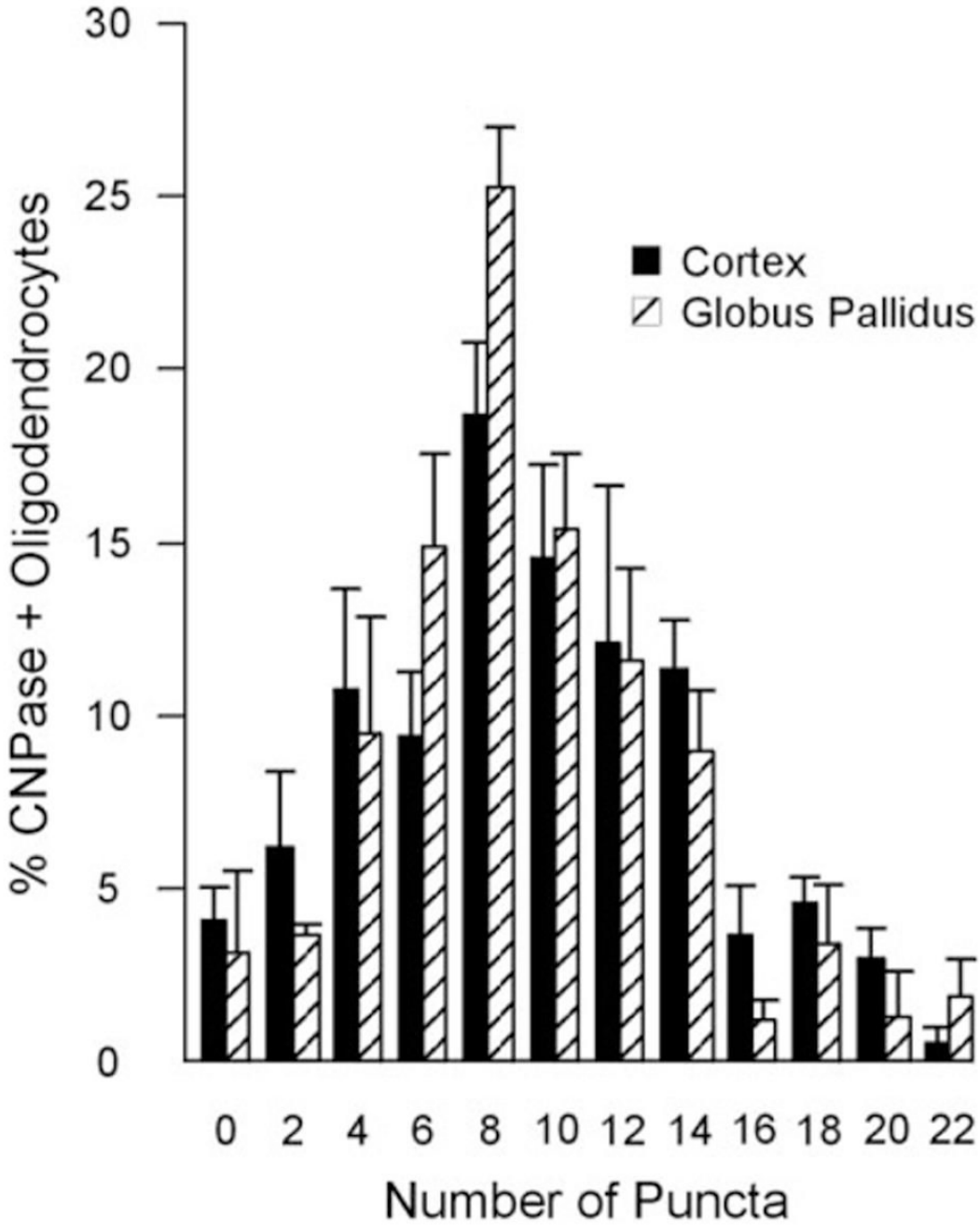

Fig. 5.

Frequency distribution showing percentage of oligodendrocytes and the numbers of Cx30-immunopositive puncta surrounding oligodendrocytes in cerebral cortex and globus pallidus. Numbers of puncta were binned in pairs (1–2), (3–4), up to (21–22). Percentages are the mean ±SE from the total number of oligodendrocytes (indicated in Table 2) examined in three WT animals.

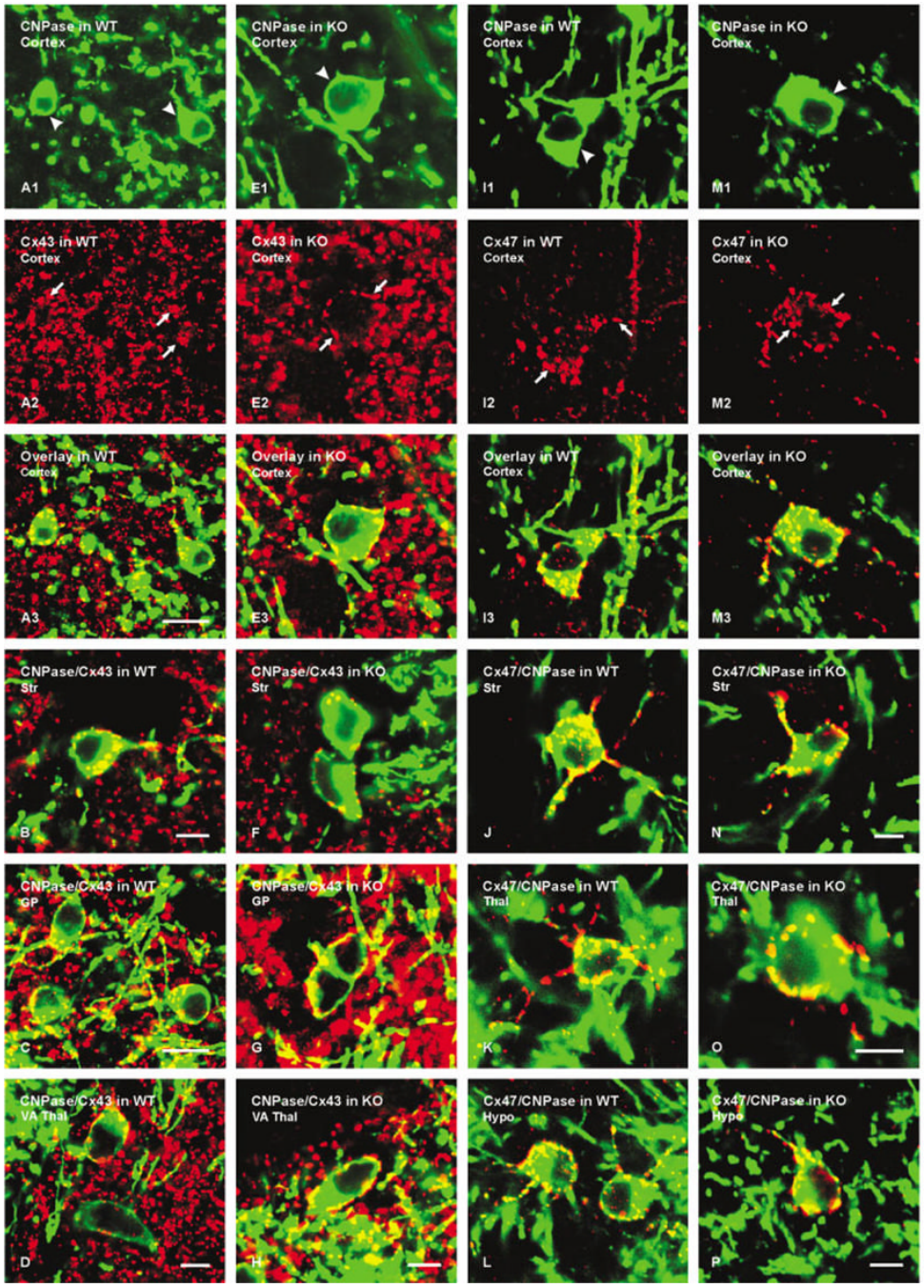

Fig. 6.

Laser scanning confocal immunofluorescence of Cx43 and Cx47 association with CNPase-labeled oligodendrocytes in various brain regions of wild-type (WT) and Cx32 knockout (KO) mice. **A**: Confocal double labeling in cerebral cortex of WT mouse showing two CNPase-positive oligodendrocytes (A1, arrowheads) with Cx43-positive puncta (A2, arrows) on the cell bodies (yellow in overlay image, A3). **B–D**: Confocal micrographs from WT mouse showing CNPase (green) co-association with Cx43 (red) as seen by yellow in overlays from striatum (B), globus pallidus (C), and ventroanterior thalamic nucleus (D). **E**: Confocal double labeling in cerebral cortex of Cx32 KO mouse showing CNPase-positive oligodendrocyte (E1, arrowheads) with Cx43-positive puncta (E2, arrows) on its surface (yellow in overlay, E3).

F–H: Confocal micrographs from Cx32 KO mouse showing CNPase (green) co-association with Cx43 (red), as seen by yellow in overlays from striatum (F), globus pallidus (G), and ventroanterior thalamic nucleus (H). *I*: Confocal double labeling in cerebral cortex of WT mouse showing a CNPase-positive oligodendrocyte (I1, arrowhead) with Cx47-positive puncta (I2, arrows) on the cell body (yellow in overlay, I3). **J–L**: Confocal micrographs from WT mouse showing CNPase (green) co-association with Cx47 (red), as seen by yellow in overlays from striatum (J), thalamus (K), and hypothalamus (L). **M**: Confocal double labeling in cerebral cortex of Cx32 KO mouse showing a CNPase-positive oligodendrocyte (M1, arrowhead) with Cx47-positive puncta (M2, arrows) on its surface (yellow in overlay, E3). **N–P**: Confocal micrographs from Cx32 KO mouse showing CNPase (green) co-localization with Cx47 (red), as seen by yellow in overlays from striatum (N), thalamus (O) and hypothalamus (P). Scale bars = 10 μm in A–C; 5 μm; in D–H,I–N,O,P.

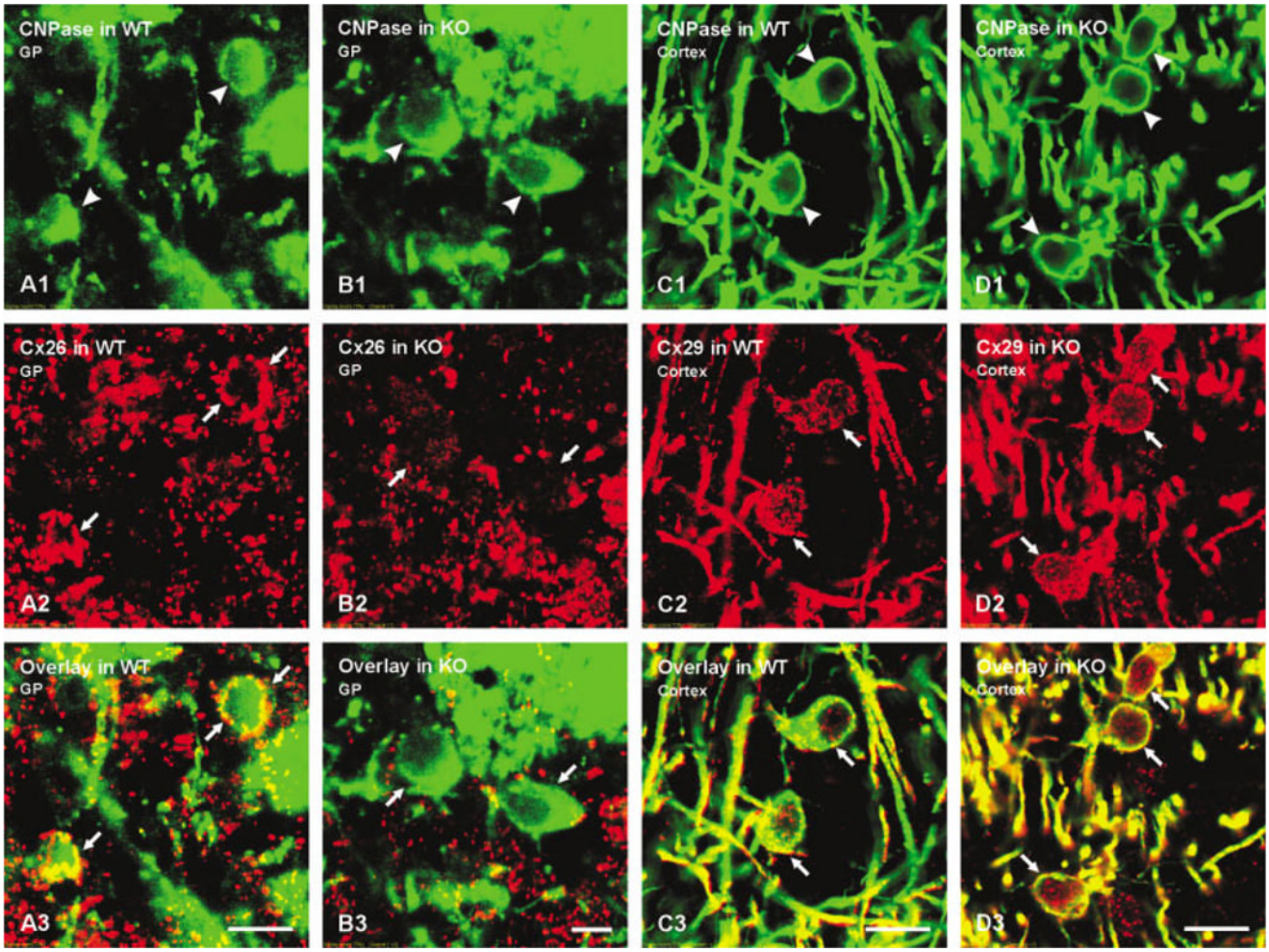

Fig. 7.

A–B: Laser scanning confocal immunofluorescence showing CNPase-positive oligodendrocytes in globus pallidus (A1,B1, arrowheads) and numerous Cx26-positive puncta on the surface of these cells in wild-type (WT) (A2, arrows), but not knockout (KO) (B2, arrows) mice as seen by yellow in corresponding overlay images (A3,B3, arrows). C,D: Laser scanning confocal immunofluorescence showing CNPase-positive oligodendrocytes in cerebral cortex (C1,D1, arrowheads), and similar appearance of Cx29 (C2,D2, arrows) associated with these cells in WT and Cx32 KO mice as seen by yellow in corresponding overlay images (C3,D3, arrows). Scale bars = 10 μm in A,C,D; 5 μm in B.

TABLE 1

Connexin Antibodies Used for Western Blotting and Immunohistochemistry*

Antibody	Type	Epitope; Designation	Reference; Source
connexin26	Monoclonal	C-terminus; 33–5800	Nagy et al., 2001; Zymed
connexin26	Polyclonal	C-terminus; 51–2800	Nagy et al., 2001; Zymed
connexin29	Polyclonal	C-terminus; 34–4200	Li et al., 2002; Zymed
connexin30	Monoclonal	C-terminus; 33–2500	Rash et al., 2001; Zymed
connexin30	Polyclonal	C-terminus; 71–2200	Nagy et al., 1999; Zymed
connexin32	Monoclonal	aa 235–246; 7C7	Li et al., 1997
connexin32	Monoclonal	C-terminus; 35–8900	Zymed
connexin32	Monoclonal	Cytoplasmic loop; 13–8200	Zymed
connexin32	Polyclonal	Cytoplasmic loop; 71–0600	Li et al., 1997; Zymed
connexin32	Polyclonal	C-terminus; 34–5700	Zymed
connexin43	Monoclonal	C-terminus; 35–5000	Zymed
connexin43	Polyclonal	C-terminus; 71–0700	Li et al., 1998; Zymed
connexin43	Polyclonal	aa 346–363; 18A	Yamamoto et al., 1990a,b
connexin47	Polyclonal	C-terminus; 36–4700	Zymed

*All antibodies were raised against peptides corresponding to connexin sequences. Monoclonal Cx32 antibody 13–8200 and polyclonal 71–0600 are directed against the same sequence in the cytoplasmic loop region of Cx32. Monoclonal 35–8900 and polyclonal 34–5700 are directed against the same sequence in the C-terminus region of Cx32. Zymed, Zymed Laboratories, South San Francisco, CA.

TABLE 2

Counts of Cx30-Immunoreactive Puncta Surrounding CNPase-Positive Oligodendrocyte Somata in Various Brain Regions of WT and Cx32 KO Mice[†]

Brain area	Wild-type	Cx32 KO
Cerebral cortex	8.96 3 0.29 (291)	1.25 3 0.07 (305)[*]
Globus pallidus	8.38 3 0.34 (165)	1.09 3 0.08 (173)[*]
VL thalamus	8.22 3 0.42 (99)	0.78 3 0.08 (153)[*]
Hypothalamus	8.14 3 0.31 (197)	0.81 3 0.06 (185)[*]

[†]Values indicate means ± SEM of the numbers of Cx30-immunopositive puncta associated with the surface of individual oligodendrocytes each viewed at a single focal plane in the indicated brain regions of wild-type (WT) and Cx32 knockout (KO) mice. Numbers in parentheses indicate the total number of oligodendrocyte somata examined in each brain region of three WT and three Cx32 KO mice.

[*]Significantly different from WT. $P < 0.001$.